MATHEMATICS CLINIC

****

Gate to Base Capacitance Modeling for Nano-scale MOSFETs

Final Report
June 2007

TO
USC – Information Sciences Institute

Clinic Team: Dwayne Chambers
Xiaoyu Che
Adam Cox
Zheng Cui

Faculty Advisor: Ellis Cumberbatch

Consultant: Hedley Morris

Liaison: Henok Abebe

Gate to Base Capacitance Modeling for Nano-scale MOSFETs

1 Introduction

The continued down-scaling of CMOS technology has brought serious deterioration in the accuracy of the SPICE(simulation program with integrated circuit emphasis) device models used in the design of chip functions. This is due in part to quantum effects that occur in modern nano-scale MOSFET devices. The focus of this paper is on modeling quantum effects based on the Density-Gradient (DG) model. In [AFY06], a first integral to the Density Gradient Equations was determined for the MOSFET in the inversion regime. In [CUA07], asymptotic expansions for the inversion region of current flow in the MOSFET were calculated. In this report parallel results for the Accumulation Region will be determined. This paper focuses on modeling gate-to-base capacitance as a function of the applied voltage.

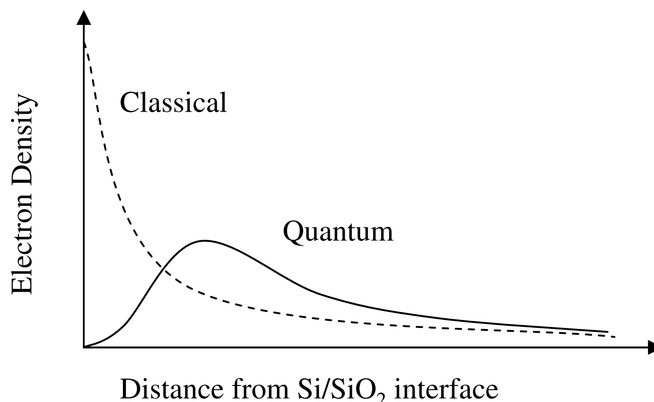

Figure 1: Comparison of classical and quantum solutions for the electron density.

A full treatment using quantum mechanics requires QM solutions in the gate metal material and in the oxide insulator, as well as in the silicon base. The oxide, having a large barrier height, would generate only a small electron density. In this case the electrons are said to have leaked or tunnelled into the oxide. In the treatment here, the electron density in the insulator is taken to be zero. The quantum treatment requires that the electron density be continuous so that the boundary condition at the oxide/silicon interface is zero electron density, whereas the classical theory based on the drift-diffusion model using the quasi 1-D approximation gives maximum charge density at this interface. This is the main discrepancy between the classical and quantum models. Several models have received attention. Full solutions of the Schrödinger and Gauss equations, and various other approximations, all require high level numerical simulations. This multi-dimensional microscopic solution is inappropriate for practical circuit application [AT87, BRYDA98].

The classical description, which is conventionally the drift-diffusion (DD) current density

model, may be obtained by assuming that the internal energy densities of the electron and hole gases have a logarithmic dependence on the charge densities. A more general series expansion of the density using the kinetic theory of gases gives that the energy depends not only on the density but also on the spatial gradient of density [AT87, AYLDV97]. This is the central assumption of the DG theory and it is derived from electron and hole kinetics by applying hydrodynamic theory. The association with quantum mechanical effects is made by interpreting the extra DG term as a quantum term, and suitably changing the boundary conditions. However, the DG model may also be generated directly from the quantum mechanics for electrons by expressing the Schrödinger wave function in amplitude/phase form(see section 2.2 of [CUA07]). The DG model has been solved numerically for a variety of devices and it has shown good accuracy compared with more complete models, in particular with quantum microscopic solutions for tunneling and confinement effects; see [AT87, p. 7964], [An90, p. 1228] and [AI89 p. 9537].

The quantum term in the DG model is higher order than the DD terms and it is multiplied by a numerically small factor. This indicates a boundary layer behavior which is confirmed by the numerical results: the inversion charge density is reduced significantly in a small layer close to the silicon/silicon-oxide interface, but the charge behavior outside this layer is similar to the non-quantum, classical solution (see Figure 1). The maximum of the classical charge distribution is shifted away from the oxide interface under the influence of quantum effects, and its value may be reduced by up to two orders of magnitude. This loss of electrons results in diminished source-to-drain current, and it affects the gate capacitance circuit element. (The shift in the maximum density may be viewed as an increased oxide thickness.) Also, in the case when the electron mobility is position dependent, an effective value is obtained by averaging with respect to the charge carrier density, and this value is amended due to the classical to quantum profile change shown in Figure 1.

In this paper the goal is to model the quantum effects on the gate-to-base capacitance a MOSFET using the results from the mid-year report (See [CCCCC07]). As these results prove insufficient, a new hybrid model is proposed based on an approximation from quantum mechanics. Much of this paper concerns itself with an analysis of this new model. The simulation program SCHRED will be used as a comparison for results from this hybrid model.

Section 2 contains a brief introduction to the drift-diffusion equations (Section 2.1), the density-gradient extension (Section 2.2), the defintion of the boundary value problem (Section 2.3), and the nondimensional scaling used (Section 2.4). Section 3 contains the analysis for obtaining a first integral of the differential equations in the accumulation regime (Section 3.1.1) together with the calculation of an unknown parameter from perturbation analysis of the inner quantum layer similar to that presented for inversion in [CUA07], (Section 3.2.1). The results for the inversion regime which were obtained in [CCCCC07] are repeated for comparison in Section 3.1.2 and 3.2.2. Section 4 introduces a new model based on estimates on the change in surface potential based on quantum mechanics, and its use in the first integrals obtained. Section 5 applies these results to the determination of the

gate-to-base capacitance, and Section 6 display the capacitance obtained from these results, alongside comparisons from the SCHRED software.

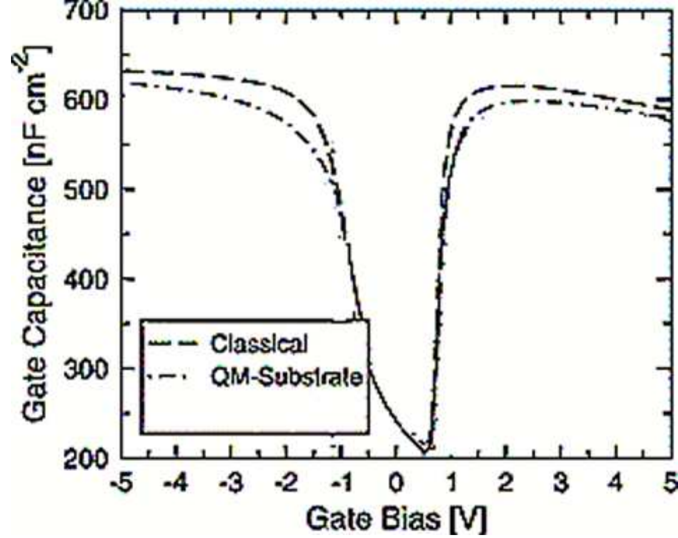

Figure 2: Comparison of classical and quantum solutions for capacitance.

2 Model Equations and Parameter Scaling

2.1 The Drift-Diffusion Equations.

The motion of electrons and holes is assumed to be governed both by the electric field and by diffusion using the standard Fick's law. This gives for the electron and hole fluxes

$$\left.\begin{array}{l} \mathbf{J}_n = q(n\mu_n\mathbf{E} + D_n\nabla n) \\ \mathbf{J}_p = q(p\mu_p\mathbf{E} - D_p\nabla p) \end{array}\right\} \tag{2.1}$$

where $\mathbf{J}_n, \mathbf{J}_p$ are the electron and hole current densities, q is the magnitude of the electronic charge, n, p are the electron and hole concentrations and D_n, D_p are the electron and hole diffusivities. The electron hole mobilities μ_n and μ_p depend in general on doping levels and the electrostatic field $\mathbf{E}$, but usually are taken as constant. With the Einstein relation:

$$D = \frac{kT\mu}{q} \tag{2.2}$$

and with

$$\mathbf{E} = -\nabla\psi$$

we can write

$$\left.\begin{array}{l} \mathbf{J}_n = n\mu_n\nabla(-\psi q + kT\ln n) = -qn\mu_n\nabla\Phi_n \\ \mathbf{J}_p = -p\mu_p\nabla(\psi q + kT\ln p) = -qp\mu_p\nabla\Phi_p \end{array}\right\} \tag{2.3}$$

where k is Boltzmann's constant, T is the lattice temperature (assumed constant), ψ is the electrostatic potential, Φ_n and Φ_p are the "electro-chemical quasi-Fermi potentials" for electrons and holes. These definitions give

$$n = n_i \exp\left[(\psi - \Phi_n)/V_{th}\right] \quad \text{and} \quad p = n_i \exp\left[(-\psi + \Phi_p)/V_{th}\right] . \tag{2.4}$$

where $V_{th} = kT/q$ is called the thermal voltage. Here n_i is a constant called the intrinsic carrier density, and it represents the density of both holes and electrons in undoped silicon. Gauss' equation for charge conservation and the conservation equations for holes and electrons can now be written

$$\begin{array}{l} \varepsilon\nabla.\mathbf{E} = -\varepsilon\nabla^2\psi = \rho = q(p - n + N) \\ \frac{\partial n}{\partial t} - \frac{1}{q}\nabla.\mathbf{J}_n = G_n - U_n \\ \frac{\partial p}{\partial t} + \frac{1}{q}\nabla.\mathbf{J}_p = G_p - U_p \end{array} \tag{2.5}$$

where ε is the material dielectric constant, and $N = N_D - N_A$ is the static doping, comprising donors and acceptors. G_n, G_p are the electron and hole generation rates, and U_n, U_p are the electron and hole recombination rates. See Sze [S81] for expressions specifying the generation and recombination terms.

Equations (2.5), together with (2.3), (2.4), constitute three non-linear partial differential equations for the potentials ψ, Φ_n and Φ_p, in the most general context. This is the standard drift-diffusion model which has been the basis for most of the technical development of the semi-conductor industry [S81, MRS 90].

In the application to current flow in an n–channel MOSFET, the holes are considered to be in thermal equilibrium, implying that Φ_p is constant, taken to be zero. Also the generation/recombination terms are omitted and only the case of time-independent currents is considered. For SPICE application this steady state approximation is good for circuits operating at frequencies less than 100MHz. For high frequency circuit applications SPICE steady state solutions are corrected by engineering approximations to include high frequency effects.

2.2 The Density Gradient Model for the Quantum Effect.

The model employed in this paper is referred to in the semi-conductor literature as the DG model. This appellation derives from continuum mechanics (see [AT87], [AI89]): extensions

from kinetic theory to the basic laws for a continuum which assume that the internal energy is a function of density give that the energy depends also on the spatial gradient of density. In the semiconductor context a similar extension to the DD model to include a quantum term may be obtained directly from the Schrödinger equation. For a brief derivation see [CUA07].

The classical quasi-Fermi potential in (2.5b), whose gradient is proportional to the force field extant in the continuum is, in the DG quantum extension, replaced by

$$\begin{aligned} \Phi_p &= \psi + V_{th}\ln(p/n_i) + \Phi_{qp} \\ \Phi_n &= \psi - V_{th}\ln(n/n_i) + \Phi_{qn} \end{aligned} \tag{2.6}$$

where

$$\begin{aligned} \Phi_{qp} &= 2b_n(\nabla^2\sqrt{p})/\sqrt{p}, \quad b_n = \hbar^2/12m^*q \\ \Phi_{qn} &= 2b_n(\nabla^2\sqrt{n})/\sqrt{n}, \quad b_n = \hbar^2/12m^*q \end{aligned}$$

in which $\hbar$ is Planck's constant. The factor m^* represents the hole, or electron, effective mass normal to the interface (the holes, or electrons, are not quantized transverse to the interface). This factor is usually used as a fitting parameter, see [AYLDV07].

2.3 The Boundary Value Problem.

Equation (2.5), amended by the assumptions discussed at the end of Section 2.1, together with equations (2.3), (2.6), relating Φ_p with p and Φ_n with n comprise the field equations in the silicon $0 < x_1 < \infty$, $0 < x_2 < L$, where L is the channel length. No variation with x_3 is considered. The silicon region is adjoined by the oxide, $-t_{ox} < x_1 < 0$, in which no charges are assumed to reside, giving $\nabla \cdot \mathbf{E}=0$ there.

The following boundary conditions on ψ and Φ_p are standard (see [WOC90]) :

$$\begin{gathered} \psi|_{x_1=-t_{ox}} = V_{GS} - V_{FB}, \;\; \psi|_{x_1\to\infty} = -V_{th}ln\ (N_A/n_i) \\ (\psi,\Phi_p)|_{x_2=0} = (V_{th}ln\ (N_A/n_i), 0) \\ (\psi,\Phi_p)|_{x_2=L} = (V_{DS} + V_{th}ln\ (N_A/n_i), V_{DS}) \end{gathered} \tag{2.7}$$

In the above V_{GS}, V_{FB} and V_{DS} are gate, flat-band and drain voltages, N_D and N_A are the source/drain and silicon doping levels, respectively, and t_{0x} is the oxide thickness. No current leaves the device across $x_1 = 0$ or at $x_1 = \infty$. Since the PDE system described above contains two more derivatives than the classical system, two extra boundary conditions must be prescribed. These are taken to be

$$n = 0\ ,\ p = 0 \;\text{ at }\; x_1 = 0 \;\text{ and }\; n \to n_i^2/N_A\ ,\ p \to N_A \;\text{ as }\; x_1 \to \infty \tag{2.8}$$

Condition (2.4) is consistent with quantum continuity of hole density and the assumption of zero density in the oxide. Condition (2.8) is adopted on the basis that, though quantum

effects alter the solution close to the gate interface region, the solution in the silicon bulk returns to its classical values. It is noted that in simulations using the full Schrödinger wave function Ψ the boundary conditions are taken to be $\Psi = 0$ at $x_1 = 0$ and at $x_1 = \infty$. The first condition is equivalent to (2.8) and the second is not dis-similar to (2.8) since n_i^2/N_A is many orders of magnitude smaller than the hole densities in the accumulation region.

2.4 Scaled Variables.

In order to facilitate the use of the MOSFET I–V results obtained in [CAM01] for the non-quantum case, we employ the scaling used there; it was introduced by Ward in [WOC90]. The scaling is

$$\begin{array}{c} (x_1, t_{ox}) = (x, t) L_D \sqrt{2(\ln\lambda)/\lambda},\ x_2 = yL, (\psi, \Phi_p) = (w, \varphi) V_{th} \ln\lambda \\ V_{DS} = V_{ds} V_{th},\ V_{GS} - V_{FB} = V_{gs} V_{th} \ln\lambda \end{array} \tag{2.9}$$

where $L_D = \left(\frac{kT\varepsilon_{si}}{2n_i q^2}\right)^{1/2}$ is called the intrinsic Debye length, and $\lambda = N_A/n_i$. This definition of L_D, in accord with current practice in the semi-conductor literature, has a $1/\sqrt{2}$ factor not present in previous publications [W0C90, W92, CAM01, AC03, AC04]. In the above, N_A is the substrate doping, typically of order $10^{15} - 10^{17} cm^{-3}$, giving $\lambda \sim 10^5 - 10^7$. The scaling in (2.9) yields $O(1)$ changes in the scaled potential over the $O(1)$ changes in x that represent the depletion depth.
The reduction to ordinary differential equations is afforded by the quasi-one-dimensional approximation, which is valid for large aspect-ratio devices ($L >>$ depletion depth), see [WOC90,CAM01].

With this scaling, the quasi-1-D drift-diffusion equations reduce to

$$\left.\begin{array}{lr} w_{xx} = 0 & \text{in} \quad -t < x < 0 \\ w_{xx} = (n-p)/N_A + 1 & \text{in} \ \ x > 0 \end{array}\right\} \tag{2.10}$$

neglect n in accumulation (and p in inversion).

The quantum revisions to n and p, equation (2.6), become

$$\begin{array}{l} w = \frac{1}{\ln\lambda} \ln\left(\frac{p}{n_i}\right) - \frac{\lambda\beta^2}{(\ln\lambda)^2} \frac{1}{\sqrt{p}} \frac{d^2\sqrt{p}}{dx^2} \\ w = \frac{1}{\ln\lambda} \ln\left(\frac{n}{n_i}\right) - \frac{\lambda\beta^2}{(\ln\lambda)^2} \frac{1}{\sqrt{n}} \frac{d^2\sqrt{n}}{dx^2} \end{array} \tag{2.11}$$

where $\beta^2 = 2b_n/V_{th}L_D^2$.

Equation (2.10) gives a linear potential in the oxide so that the continuity of electrostatic potential and displacement at the silicon/silicon dioxide interface yield boundary conditions

there for equations (2.8)-(2.10) as

$$n = 0 \text{ or } p = 0 \text{ and } \frac{\partial w}{\partial x} = c(w - V_{gs}) \text{ at } x = 0 \tag{2.12}$$

where $c = \sqrt{2\ln\lambda/\lambda}\epsilon_{ox}L_D/\epsilon_{si}t_{ox}$ and $\varepsilon_{si}, \varepsilon_{ox}$ are the dielectric constants of silicon and silicon dioxide.

Classical boundary conditions in the silicon bulk are

$$n \to \frac{n_i^2}{N_A}, \; p \to N_A, \text{ and } w \to -1 \text{ as } x \to \infty. \tag{2.13}$$

It is assumed that quantum effects do not change conditions in the bulk. Hence, the asymptotic values (2.13) are also taken by the quantum solution. In (2.11) the factor $\beta^2\lambda/(\ln\lambda)^2$ is $O(10^{-4})$ for $\lambda = 10^7$. This indicates that the quantum correction term is significant in a layer much smaller than the depletion length and a fraction of the length scale of the inversion or accumulation layers. Outside this narrow quantum layer this term has the effect of shifting the classical solution away from the interface. Numerical solutions confirm this behavior showing that the QM effect on the electron density is substantial in a narrow layer close to the oxide interface, reducing it from high values to zero at the interface. (See Figure 1). The electron or hole density is zero at the oxide interface with the charge peak at $5\mathring{A}$ to $15\mathring{A}$. The solution of (2.11) in this narrow layer is called the inner solution.

3 First Integral

Next we derive a first integral from the governing equations described above. A first integral has already been obtained by last year's Clinic team (See [AFY06]) for the inversion region. Here, a similar procedure is used in order to obtain a first integral for the accumulation region.

3.1.1 Accumulation

The equations modeling the scaled surface potential are given by (2.10) together with (2.11). For notational purposes, the substitution $b^2 = p$ is made. Multiplying (2.11) by w' and (2.10) by bb' the equations can be rewritten as

$$b^2 w' = N_A(w' - w'w'') + w'n. \tag{3.1}$$

$$bb' - bb'w = \frac{2bb'}{\ln\lambda}\ln\left(\frac{b}{\sqrt{n_i}}\right) - \frac{\lambda\beta^2}{(\ln\lambda)^2}b'b''. \tag{3.2}$$

Note that given a function f, the expression ff' and be rewritten as $\left(\frac{f^2}{2}\right)'$, by use of the Chain Rule. The resulting equations are

$$\begin{aligned} b^2 w' &= N_A(w' - (\frac{(w')^2}{2})') + w'n, \\ \left(\frac{b^2}{2}\right)' - bb'w &= \frac{1}{2\ln\lambda}\left(2b^2\ln\frac{b}{\sqrt{n_i}} - b^2\right)' - \frac{\lambda\beta^2}{(\ln\lambda)^2}\left(\frac{(b')^2}{2}\right)'. \end{aligned}$$

Multiplying the first equation by $\frac{1}{2}$ and subtracting the second allows all terms to be expressed as a derivative. Integration yields the first integral in the accumulation region

$$\frac{b^2 w}{2} - \frac{b^2}{2} = \frac{N_A}{2}(w - \frac{(w')^2}{2}) + \frac{n_i e^{(w-1)\ln\lambda}}{2\ln\lambda} + \frac{\lambda\beta^2}{(\ln\lambda)^2}\frac{(b')^2}{2} - \frac{1}{2\ln\lambda}\left(2b^2\ln\frac{b}{\sqrt{n_i}} - b^2\right) + I_{CA},$$

where I_{CA} is the integration constant. Denoting the subscript $'s'$ to represent values taken at $x = 0$ and using the boundary conditions from equation (2.12), the resulting first integral is

$$(w_s')^2 = 2w_s + \frac{2n_i e^{(w_s-\phi)\ln\lambda}}{N_A\ln\lambda} + 2\frac{\lambda\beta^2}{(\ln\lambda)^2}(b'(0))^2 + \frac{2I_{CA}}{N_A}. \tag{3.3}$$

The integration constant is calculated on the assumption that the quantum effects disappear at infinity and the variables return the to the classical values. Using the asymptotic values at infinity allows for the calculation that

$$\frac{I_{CA}}{N_A} = 1 - \frac{1}{\lambda\ln\lambda} - \frac{1}{\lambda^2\ln\lambda}.$$

3.1.2 Inversion

Using the same methods in the previous section a derivation of the first integral for the Inversion region was accomplished by the clinic team of 2005-2006 (See [AFY06]). The result is that

$$(w_s')^2 = 2\left(w_s + \frac{e^{-w_s\ln\lambda}}{\lambda\ln\lambda} + \frac{(a'(0))^2\beta^2\lambda}{N_A(\ln\lambda)^2} - \frac{I_{CI}}{N_A}\right), \tag{3.4}$$

for $a^2 = n$ and $\frac{I_{CI}}{N_A} = -\frac{I_{CA}}{N_A}$ is the integration constant. Note that w_s' satisfies the following inequalities in the differente regions

$$\begin{aligned} w_s' &> 0 \text{ in accumulation} \\ w_s' &< 0 \text{ in inversion} \end{aligned} \tag{3.5}$$

which informs whether the positive or negative square root is needed in each region.

3.2 Estimating $a'(0)$ and $b'(0)$

The difficulty in these quantum equations is that they contain $a'(0)$ and $b'(0)$. Explicit formulae do not exist for these terms. Using the perturbation introduced in [CUA07] and deriving the inner and outer solutions will produce an estimate for these terms.

3.2.1 Procedure for $b'(0)$

In order to evaluate the the relationship between w_s and w'_s in the first integral (3.3) the value for $b'(0)$ is needed. Following Section ?? in [CUA07] we extract b from the relation between the T and the concentration of holes, p

$$T = \sqrt{\frac{p}{n_i}}$$

where $b = \sqrt{p}$. From this equation we see that $b'(0)$ equals $\sqrt{n_i}T'(0)$. The expansion used is

$$\sqrt{p/n_i} = T = T_0 + \delta T_1 + \cdots$$

where $\delta^2 = \frac{\lambda\beta^2}{2\ln\lambda}$, and so,

$$b'(0) = \sqrt{n_i}[\frac{1}{\delta}\frac{dT_0}{dX}|_{X=0} + \frac{dT_1}{dX}|_{X=0}] \tag{3.6}$$

As in the analogous procedure for finding $a'(0)$ in inversion in [CCCCC07] it is noted that

$$T_1 = \frac{1}{2}\ln\lambda T_0 Y_1 \tag{3.7}$$
$$T_0 = \tau_{0s} S_0 \tag{3.8}$$

Substituting in [CCCCC07] equation (3.11)

$$T_0'' - T_0\ln T_0 - \ln\lambda\,(W_0 - 1)\,T_0/2 = 0, \tag{3.9}$$

and noting that given $T_0(\infty) = e^{\frac{1}{2}(1-w_s)ln\lambda}$, then $w_{0s} = 1 - \frac{2lnT_0(\infty}{ln\lambda}$, (3.9) becomes

$$T_0'' - T_0\ln T_0 + T_0 lnT_0(\infty) - \frac{T_0}{2}\ln\lambda s_0 X = 0. \tag{3.10}$$

Further rearranging, substituting $X = 0$ and assuming $T_0(\infty) = \tau_{0s}$ yields

$$S_0''\tau_{0s} - S_0\tau_{0s}\ln(S_0\tau_{0s}) + S_0\tau_{0s}\ln\tau_{0s} = 0, \tag{3.11}$$

which when simplified and divided thru by τ_{0s} becomes:

$$S_0'' = S_0 \ln S_0. \tag{3.12}$$

And

$$X = \int_0^{S_0} (s^2 \ln s + (1 - s^2)/2)^{-1/2} ds, \tag{3.13}$$

$S_0(0) = 0$, so

$$\frac{dX}{dS_0}|_{X=0} = (S_0^2 \ln S_0 u + \frac{1 - S_0^2}{2})^{-1/2} = (\frac{1}{2})^{-1/2} = \sqrt{2}. \tag{3.14}$$

It follows that

$$\frac{dT_0}{dX}|_{X=0} = \frac{1}{\sqrt{2}} \tau_{0s}. \tag{3.15}$$

This concludes determining the first half of (3.6). Attention is now turned to determining the second half, $\frac{dT_1}{dX}$ evaluated at $X = 0$.

Given equation (3.7), differentiating produces the following relation:

$$\frac{dT_1}{dX} = \frac{1}{2} \ln \lambda (\frac{dT_0}{dX} Y_1 + T_0 \frac{dY_1}{dX}). \tag{3.16}$$

The following two equations are derived from [CUA07]. The only modification being in the instance of accumulation there is a sign change for W_{1s}.

$$Y_1'' + 2(S_0'/S_0)Y_1' - Y_1 = W_{1s} - S_1 X \tag{3.17}$$

$$\begin{aligned} Y_1 = \; & \tfrac{1}{3} \quad e^{-X}(1 - e^X)^{-1}\{E_1(1 + 3e^X) + E_2(1 + e^X)^3 + W_{1s}(2 + 3e^X + 3e^{2X}) \\ + \; & s_1(2e^X + 2e^{2X} + 3Xe^X + 3Xe^{2X} + 2Xe^{3X} \\ - \; & 2(1 + 3e^X + 3e^{2X} + e^{3X}) ln(1 + e^X))\} \end{aligned} \tag{3.18}$$

Since the E_2 term is exponentially large at $X >> 1$, we have $E_2 = 0$. Hence

$$E_1 = -2W_{1s} + s_1(1 - 4ln2) \tag{3.19}$$

Using L'Hopital's Rule,

$$Y_1|_{X=0} \rightarrow -W_{1s} + S_1(12ln2 - 3) \tag{3.20}$$

And applying L'Hopital's Rule twice, the following is obtained:

$$\frac{dY_1}{dX}|_{X=0} = 0.$$

Combining the above results in (3.16),

$$\frac{dT_1}{dX} = \frac{1}{2}\ln\lambda(\frac{1}{\sqrt{2}}\tau_{0s}(-W_{1s} + S_1(12\ln 2 - 3)). \tag{3.21}$$

Combining the above results in equation (3.6) gives the following result:

$$\begin{aligned} b'(0) &= \sqrt{n_i}\frac{1}{\delta}\frac{dT}{dX}|_{X=0} \\ &= \sqrt{n_i}\left[\frac{1}{\delta}\frac{dT_0}{dX}|_{X=0} + \frac{dT_1}{dX}|_{X=0}\right] \\ &= \sqrt{n_i}\left\{\frac{1}{\delta}\frac{1}{\sqrt{2}}\tau_{0s} + \left[\frac{1}{2}\ln\lambda\left(\frac{1}{\sqrt{2}}\tau_{0s}(-W_{1s} + S_1(12\ln 2 - 3))\right)\right]\right\} \end{aligned} \tag{3.22}$$

3.2.2 Procedure for $a'(0)$

The parallel result is determined in [CCCCC07] for the Inversion region. The same procedure was used to obtain this result as in the above equation.

$$a'(0) = \sqrt{n_i}\left\{\frac{1}{\delta}\frac{1}{\sqrt{2}}\tau_{0s} + \left[\frac{1}{2}\ln\lambda\left(\frac{1}{\sqrt{2}}\tau_{0s}(W_{1s} + S_1(12\ln 2 - 3))\right)\right]\right\} \tag{3.23}$$

3.3 Analysis and Simulations

Using the estimates described in Sections 3.2.2 and 3.2.1 proved unsatisfactory when simulations were run. They deviated considerably from intuition based on quantum theory and SCHRED simulations. The difficulty was that the estimates grew too rapidly as the surface potential increased. This is most likely due to the fact that there are two small parameters working together. One of these terms describes the inner layer of the solution and the other is the quantum parameter. To get a more accurate estimation, a perturbation in two parameters might be an option, however, this is extremely difficult and quite impractical. Instead, a hybrid model is considered to achieve a new estimate of the needed terms.

4 The New Model

We consider a new hybrid model based on the difference in surface potential between the classical and quantum models. This change is developed in [CA04] and denoted Δ, which expresses the change in energy gap due to the QM effects (See also [RAHKFG07] and [VWW94]).

4.1 The Delta Parameter

The first integral method used in Section 3 was not satisfactory, so there was a need to introduce this new hybrid model which is based on the channel surface potential.

The parameter w_{qs} is the scaled surface potential by the outer solution at the silicon/silicon-oxide interface, and its magnitude is less than the magnitude of the classical surface potential. The relation is given by $w_{qs} = w_s - \Delta$, where Δ is defined below.

The surface potential expression is usually determined by solving the Poisson equation with boundary conditions at the interface and substrate. The Poisson equation for NMOS is written as

$$V'' = \frac{q}{\varepsilon_s}[n - p + N_A] \tag{4.1}$$

It is possible to get an expression for w_{qs} from the interface boundary condition of the outer solution by considering the quantum layer thickness as part of the oxide thickness. The classical charge density n in (4.1) is corrected by modeling the quantum effects on the semiconductor band gap, see references above, and this leads to

$$w_{qs} = w_s - \Delta = w_s - \frac{\Delta E_g}{2k_bT\ln\lambda}. \tag{4.2}$$

The term ΔE_g is the change in the energy gap due to quantum effects and is given by the following relation:

$$\Delta E_g = \frac{13}{9}\beta(\frac{\varepsilon_s}{4k_bT})^{\frac{1}{3}}(\frac{V_{gs}+V_T}{6t_{ox}^q})^{\frac{2}{3}}$$

where $\beta = 6.6 \times 10^{-29}$ J-m, k_b is the Boltzmann constant, T temperature, and t_{ox}^q is the enhanced oxide thickness. In [RAHKFG07] t_{ox}^q is found by matching the data and its value given by the oxide thickness plus 0.7nm and V_T is a threshold voltage given as 0.0259 volts. The term Δ above is non-dimensional and the scaling introduced in Section 2.4 results in

$$\Delta = \frac{\Delta E_g}{2k_bT\ln\lambda} = \frac{13}{9}\beta(\frac{\varepsilon_s}{4k_bT})^{1/3}(\frac{\bar{V}_{gs}+\bar{V}_T}{6\bar{t}_{ox}^q})^{2/3}(\frac{V_{th}\ln\lambda}{L_D(\frac{2\ln\lambda}{\lambda})^{1/2}})^{2/3}\frac{1}{2k_bT\ln\lambda}$$
$$= \frac{13}{36}\frac{1}{2^{1/3}3^{2/3}}\frac{\beta\lambda^{1/3}}{(\ln\lambda)^{2/3}}\frac{n_i^{1/3}}{qV_{th}}(\frac{\bar{V}_{gs}+\bar{V}_T}{\bar{t}_{ox}^q})^{2/3}$$

where the bar over a variable denots its scaled value so that $(\frac{\bar{V}_{gs}+\bar{V}_T}{\bar{t}_{ox}^q})^{2/3}$ is now non-dimensional. The unit of β is J-m (the units of energy), qV_{th} is also measured in units of energy, and $(n_i)^{1/3}$ has a dimension of $length^{-1}$, so $\beta\frac{n_i^{1/3}}{qV_{th}}$ is non-dimensional, hence Δ is non-dimensional.

4.2 Including Delta in the First Integral

Using the work in Sections 3.2.2 and [CUA07] a formula for $a'(0)$ can be derived. Equation (3.38) in [CUA07] gives the relation that

$$\sqrt{\frac{n}{n_i}} = T_0 = \tau_{0s}S_0.$$

With this, and equation (3.39) in [CUA07] the explcit formula for $a'(0)$ is found to be

$$a'(0) = \sqrt{\frac{n_i}{2}}\frac{1}{\delta}e^{\frac{w_{gs}\ln\lambda}{2}} \tag{4.3}$$

Substituting this back into (3.4) a first integral involving Δ is derived.

$$\frac{1}{2}(w_s')^2 = \frac{1}{\ln\lambda}\left(e^{(w_s-\Delta-1)\ln\lambda} + e^{-(w_s+1)\ln\lambda}\right) + w_s - \frac{I_{CI}}{N_A}. \tag{4.4}$$

Note that (4.4) is almost identical to the solution to the classical model under the drift diffusion equations described in Section (2.1). The difference lies in the presence of Δ and it finds itself in the term which represents the presence of electrons. Solutions to (4.4) we will denote by U_s, the surface potential in the quantum case, and w_{sc} will be the surface potential in the classical case.

5 Capacitance

In order to plot results, it was necessary to express both capacitance, C and gate voltage V_{gs} in terms of w_s, for both classical and quantum scenarios. In addition this made it possible to relate capacitance to gate voltage in order for final plots to be made.

The following are relations, already determined, and by which an expression for capacitance C and gate voltage V_{gs} in terms of w_s could be discovered. Note that we use Q to denote the total charge in the substrate, so that

$$Q = \int_0^\infty w'' dx = -w'_s$$

Hence, from (2.12)

$$Q = -w'_s = c(V_{gs} - w_s)$$

The capacitance is the derivative of the total charge with respect to applied voltage, so that

$$C = \frac{dQ}{dV_{gs}} = c(1 - \frac{dw_s}{dV_{gs}}) \tag{5.1}$$

Note: We are using scaled variables. The analysis completed above gives relationships (classical or quantum) between w'_s and w_s. Representing these by,

$$\tfrac{1}{2}w_s'^2 = \tfrac{1}{2}Q^2 = G(w_s) \text{ note this means } Q = \sqrt{2G(w_s)},$$

$$\Rightarrow Q\frac{dQ}{dw_s} = \frac{dG}{dw_s} = F(w_s)$$

$$\Rightarrow \frac{dQ}{dw_s} = \frac{1}{Q}\frac{dG}{dw_s} = \frac{F(w_s)}{Q} \tag{5.2}$$

Classical Case - Equations (Inversion Only)

$$w'' = F(w_s) = e^{(w_{sc}-1)ln\lambda} - e^{-(w_{sc}+1)ln\lambda} + 1 \tag{5.3}$$

and

$$G(w_s) = \frac{1}{2}w_s'^2 = \frac{1}{ln\lambda}e^{(w_{sc}-1)ln\lambda} + \frac{1}{ln\lambda}e^{-(w_{sc}+1)ln\lambda} + w_{sc} - \frac{I_{CI}}{N_A} \tag{5.4}$$

5.1 Classical Procedure

Starting from the relation in (5.1) a substitution is made. A new expression for the capacitance is derived to be

$$C = c(1 - \frac{1}{1 + \frac{1}{c}\frac{dQ}{dw_s}}) = \frac{\frac{dQ}{dw_s}}{1 + \frac{1}{c}\frac{dQ}{dw_s}}$$

Substituting (5.2) then yields,

$$C = \frac{cF(w_s)}{cQ + F(w_s)} \tag{5.5}$$

or

$$\frac{1}{C} = \frac{Q}{F(w_s)} + \frac{1}{c} = \frac{\sqrt{2G(w_s)}}{F(w_s)} + \frac{1}{c}. \tag{5.6}$$

From (**??**)

$$V_{gs} = w_{sc} + \frac{1}{2}\sqrt{2G(w_s)}. \tag{5.7}$$

Explicitly these relations are:

$$\frac{1}{C} = \frac{\sqrt{2(\frac{1}{ln\lambda}e^{(w_{sc}-1)ln\lambda} + \frac{1}{ln\lambda}e^{-(w_{sc}+1)ln\lambda} + w_{sc} - \frac{I_{CI}}{N_A})}}{e^{(w_{sc}-1)ln\lambda} - e^{-(w_{sc}+1)ln\lambda} + 1} + \frac{1}{c} \tag{5.8}$$

and

$$V_{gs} = w_{sc} + \frac{1}{2}\sqrt{2(\frac{1}{ln\lambda}e^{(w_{sc}-1)ln\lambda} + \frac{1}{ln\lambda}e^{-(w_{sc}+1)ln\lambda} + w_{sc} - \frac{I_{CI}}{N_A})} \tag{5.9}$$

5.2 Quantum Procedure

In the quantum case the main relations are stated below:

$$G(w_s) = \frac{1}{2}\left(w_s'\right)^2 = w_s + \frac{e^{-w_s \ln\lambda}}{\lambda \ln\lambda} + \frac{a'(0)^2\beta\lambda}{N_A(\lambda)^2} - \frac{I_{CI}}{N_A} \tag{5.10}$$

where, from (3.23),

$$a'(0) = \sqrt{n_i}\left\{\frac{1}{\delta}\frac{1}{\sqrt{2}}\tau_{0s} + \left[\frac{1}{2}\ln\lambda\left(\frac{1}{\sqrt{2}}\tau_{0s}(W_{1s} + S_1(12\ln 2 - 3))\right)\right]\right\}$$

A more useful relation...

As alluded to in section 3, it was found that the above expression for $a'(0)$ was not suitable for determining an accurate expression for the quantum surface potential and hence capacitance. A suitable replacement was found in the relation

$$w_{qs} = w_s - \Delta \tag{5.11}$$

where Δ is given by (4.2) and $a'(0)$ by (4.3).

The following is notation used throughout this report and repeated here for clarity:

- w_{qs} - The surface potential (outer solution),
- U_s - The actual surface potential taken in the quantum solution,
- w_{sc} - The classical surface potential,
- Note that $w_{qs} \leq w_{sc} \leq U_s$,

Now the appropriate substitutions are made in the original relations...

$$Q^2 = 2G(U_s, \Delta) = 2[\frac{1}{ln\lambda}e^{(U_s-\Delta-1)ln\lambda} + \frac{1}{ln\lambda}e^{-(U_s+1)ln\lambda} + U_s - \frac{I_{CI}}{N_A}] \tag{5.12}$$

and U_s replaces w_s in equations (5.6)-(5.8). This gives the expression for capacitance in the quantum case.

$$C = \frac{\frac{dQ}{dU_s}}{\frac{dV_{gs}}{dU_s}} = \frac{\frac{\partial G}{\partial U_s} + \frac{\partial G}{\partial \Delta}\frac{d\Delta}{dV_{gs}}}{Q + \frac{1}{c}\frac{\partial G}{\partial U_s}} \tag{5.13}$$

In the inversion case the term relating the holes may be ignored, leading to the following relation

$$C = \frac{\frac{1}{\ln\lambda}e^{(U_s-\Delta)\ln\lambda}[1 - \frac{d\Delta}{dV_{gs}} + \lambda e^{-(U_s-\Delta)\ln\lambda}]}{\frac{1}{c}\frac{1}{\ln\lambda}e^{(U_s-\Delta)ln\lambda}[1 + c\lambda e^{-(U_s-\Delta)\ln\lambda} + c\sqrt{\frac{2\lambda}{\ln\lambda}e^{-(U_s-\Delta)\ln\lambda} + (U_s - \frac{I_{CI}}{N_A})\lambda^2 e^{-2(U_s-\Delta)\ln\lambda}}].} \tag{5.14}$$

Note:
$$\frac{1}{\ln\lambda}e^{(U_s-\Delta)\ln\lambda} = \ln\lambda[\frac{1}{2}c^2(V_{gs}-U_s)^2 - U_s + \frac{I_{CI}}{N_A}] = H\ln\lambda$$

where the function H is used merely for compactness. This leads to the explicit expression for quantum capacitance,

$$C = \frac{c[1-\frac{d\Delta}{dV_{gs}}+\frac{1}{H\ln\lambda}]}{1+\frac{c}{H\ln\lambda}[2H+(U_s-\frac{I_{CI}}{N_A})]^{\frac{1}{2}}+c\lambda^2 H\ln\lambda} \tag{5.15}$$

5.2.1 Strong Inversion Capacitance with Delta

First we present an analysis of the delta parameter approach. Under the assumptions of Strong Inversion, all terms (3.4) may be dropped except for the term involving the electrons. With this approximation, the capacitance in strong inversion is expected to be

$$C = \frac{c\left(1-\frac{d\Delta}{dV_{gs}}\right)}{1+c\sqrt{\frac{2}{\ln\lambda}}e^{-\frac{1}{2}(U_s-1-\Delta)\ln\lambda}}. \tag{5.16}$$

Another simplification can be made since the exponential term is negligible, leaving simply the term involving $\frac{d\Delta}{dV_{gs}}$. The derivative is calculated explicitly to be

$$\frac{d\Delta}{dV_{gs}} = \frac{2}{3}k(V_{gs}+V_{th})^{-\frac{1}{3}} \tag{5.17}$$

where k is the term representing all of the constants in the Δ parameter. Equation (5.16) and (5.17) show that as $V_{gs}\to\infty$, the classical and quantum capacitance both converge to the constant c. Hence the final results should evidence this behavior.

5.2.2 Capacitance in Accumulation Region

The following is a brief analysis of the capacitance relation in the accumulation region beginning with the adjusted formula for Δ in this region,

$$\Delta E_g = \frac{13}{9}\beta(\frac{\varepsilon_s}{4k_bT})^{\frac{1}{3}}(\frac{V_{gs}+1.5V_T-\alpha}{7.5t_{ox}^q})^{\frac{2}{3}}$$

where $\alpha = 0$ for p+ poly and $\alpha = 2.3$ for n+ poly. We use the latter.

Note that for accumulation, $U_s \leq w_s \leq w_{qs} \leq 0$. So the first integral for quantum case will be expressed by the following formula:

$$Q^2 = 2G(U_s, \Delta) = 2[\frac{1}{ln\lambda}(e^{(U_s-1)ln\lambda} + e^{-(U_s+\Delta+1)\ln\lambda}) + U_s - \frac{I_{CI}}{N_A}] \tag{5.18}$$

Following the same procedure as the inversion case, and ignoring the electron term, we obtain that:

$$C = \frac{c(1 + \frac{d\Delta}{dV_{gs}} - \lambda e^{(U_s+\Delta)\ln\lambda})}{1 - \lambda e^{(U_s+\Delta)\ln\lambda} - c\sqrt{\frac{2\lambda}{\ln\lambda}e^{(U_s+\Delta)\ln\lambda} + (U_s - \frac{I_{CI}}{N_A})\lambda^2 e^{2(U_s+\Delta)\ln\lambda}}} \tag{5.19}$$

6 Results

The next task is to produce results, expessed in graphical form, based on the formulas in this paper and compare them to data. SCHRED simulations are used for comparison because they are widely considered to be an industry standard. SCHRED is a simulation program that solves the Schrödinger and Poisson equations. It is important to mention that SCHRED implements the Fermi-Dirac Statistics for its models. So far in this paper Boltzman Statistics have been chosen and this may produce a slight discrepancy between our results and results from SCHRED; however, this discrepancy is expected to be negligible at strong inversion. In Figure 3 the plots from SCHRED using Fermi-Dirac Statistics are compared against the delta-based model adopted in Section 4. Figure 2 shows that the quantum and classical curves converge together as the voltage goes to zero. This behavior is not demonstrated either by SCHRED or the results seen in Figure 3. Analysis from Section 4.2 is consistent with Figure 3; namely, that as $V_{gs} \to \infty$ the quantum and classical capacitance converge to the constant c. This result is an application of equations (5.19) and (5.20). The limitations of the delta-based approach adopted here so far is that it is applicable only to strong inversion. We see that the results in this region ($V_{gs} > 1$) are very accurate in comparison with SCHRED. For this method to achieve convergence as $V_{gs} \to 0$ a variation in the approach is neccessary (see the next paragraph). Alternatively, a piecewise delta function may be needed.

In Figure 4, the same equations were used but a slightly different method. This is possible because given a voltage, solving (5.15) requires us to find a surface potential w_s. The relationship shared between V_{gs} and w_s is implicit and to invert this relationship would be done with the use of the Lambert Function. Hence, recursion is used to solve for the surface potential given a voltage. The method employed to produce Figure 4 is to replace

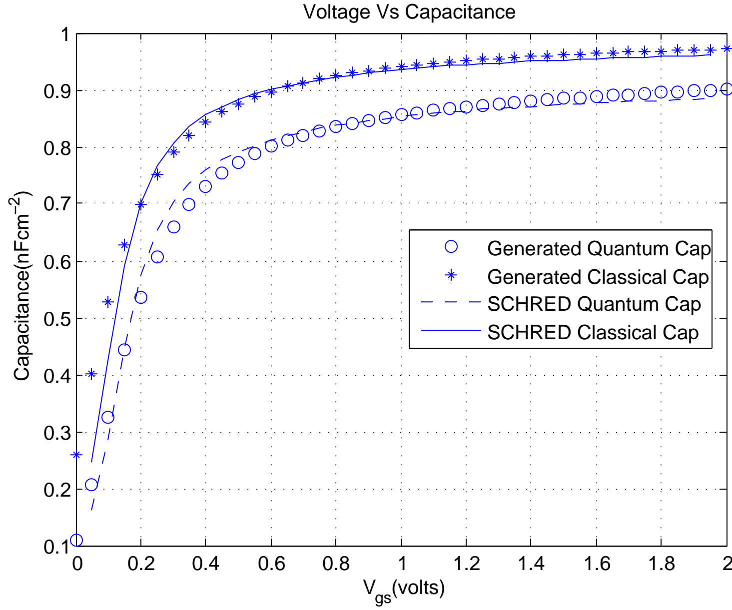

Figure 3: Comparison of classical and quantum solutions for the gate-to-base capacitance with $t_{ox} = 3.5nm$, $N_A = 10^{17}/cm^3$. The quantum capacitance is generated by eq. (5.18).

every surface potential in the quantum model with the surface potential from the classical result except for the term which represents the electrons, and hence Δ. To get a better idea of how this was accomplished, the code has been attached in Appendix A. This produces very convincing results when considering Figure 2 and ignoring the data from SCHRED. Clearly, it deviates considerably from the SCHRED data but the fact that the two converge as $V_{gs} \to 0$ is consistent with Figure 2. This method is partially justifiable since quantum effects mainly affect electrons. A complete and sure justification for using such an approach is still being contemplated and worked on; however, the fact that we have convergence as $V_{gs} \to 0$ is mathematically consistent with the equations and this new approach. This is a result of the fact that Δ is an increasing function. If the classical values are used for the surface potential, then finding the surface potential involved in the electron term will be close to the classical surface potential since $\Delta \approx 0$. Without this, the order of w_s relative to Δ becomes important and hence they will not converge unless $V_{gs} = 0$, as seen in Figure 3.

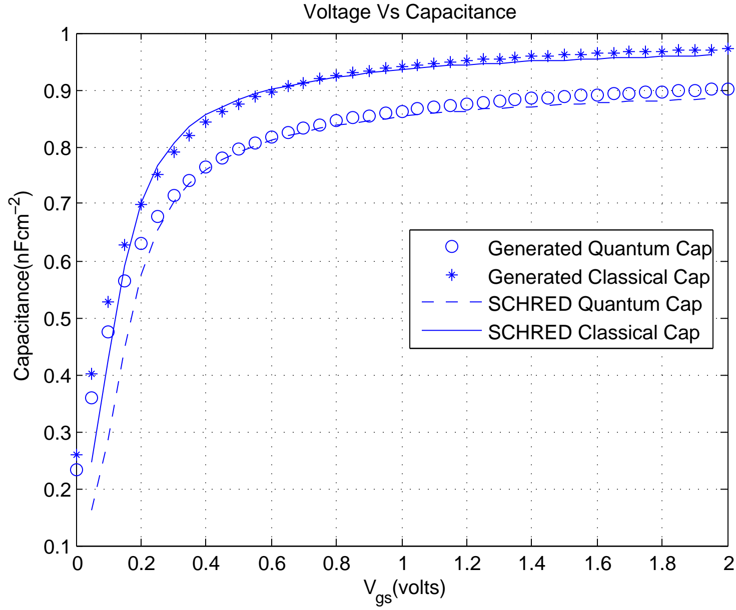

Figure 4: Comparison of classical and quantum solutions for the gate-to-base capacitance with $t_{ox} = 3.5nm$, $N_A = 10^{17}/cm$. The quantum capacitance is generated by the method explained in the text and in the code given in Appendix A.

7 Further Work

This new hybrid model is only as good as the Δ function which is chosen. Although the bulk of the work has been done for the inversion region, using a similar Δ for the Accumulation region will produce parallel results due to the fact that the solutions in the two regions share many common terms. Note, however, that if a piecewise Δ function is chosen, a blending between regions will be required. Looking at the big picture, the crux of our problems arise from finding a good estimate for $a'(0)$ and $b'(0)$. Continued examination of these two terms is what must be focused on, if this model is persisted with, in order to achieve better results.

References

[AC03] H. Abebe and E. Cumberbatch, Quantum mechanical effects corrections models for inversion charge and current-voltage (I-V) characteristics of the MOSFET device. Proceedings (2003) Nanotechnology Conference, vol. 2, pp. 218-221, San Francisco, USA.

[AC04] H. Abebe and E. Cumberbatch, Modeling quantum effects on MOSFET channel surface potential. Proceedings (2004) International Conference on Computing, Communications and Control Technologies: CCCT'04, vol. 7, pp. 198-201, Austin, Texas, USA.

[AFY06] L. Avila, M. Franklin, and D. Yong, Quantum corrections to threshold voltages for decanano MOSFETs. Submitted to USC-Information Sciences Institute, May 2006.

[AT87] M. G. Ancona and H.F. Tiersten, Macroscopic physics of the silicon inversion layer. Phy. Rev. B, vol. 35, No. 15, May (1987).

[AYLDV97] M.G. Ancona, Z. Yu, W. C. Lee, R. W. Dutton and P. V. Voorde, Density-Gradient simulations of quantum effects in ultra-thin-oxide MOS structures. IEEE Proceedings. Simulation of Semiconductor Processes and Devices, International Conference, SISPAD'97, pp. 97-100, (1997).

[A90] M.G. Ancona, Asymptotic structure of the density-gradient theory of quantum transport. Proc. Comp. Elec. Workshop, Champaign-Urbana, IL (1990).

[An90] M.G. Ancona, Macroscopic description of quantum-mechanical tunneling. Phy. Rev. B, vol. 42, No. 2, July (1990).

[AI89] M.G. Ancona and G.J. Iafrate, Quantum correction to the equation of state of an electron gas in a semiconductor. Phy. Rev. B, vol. 39, No. 13, May (1989).

[BO99] C. M. Bender and S. A. Orszag, Advanced Mathematical Methods for Scientists and Engineers, Springer-Verlag, New York, 1999.

[BRYDA98] B.A. Biegel, C. S. Rafferty, Z. Yu, R. W. Dutton, and M. G. Ancona, Simulation of ultra-small MOSFETs using a 2-D quantum-corrected drift-diffusion model. 35th Annual Technical meeting of Society of Engineering Science, pp. 53-64. September 27-30, Pullman, Washington, (1998).

[CA04] E. Cumberbatch and H. Abebe, Modeling Quantum Effects on MOSFET Channel Surface Potential. Computing, Communications and Control Technologies, vol. 7, pp. 198-201, (2004).

[CAM01] E. Cumberbatch, H. Abebe, and H. Morris, Current-voltage characteristics from an asymptotic analysis of the MOSFET equations. J. of Engineering Mathematics, vol. 39, pp. 25-46, (2001).

[CCCCC07] E. Cumberbatch, D. Chambers, X. Che, and A. Cox, Z. Cui, Modeling Capacitance for Nano-Scale MOSFETs. Submitted to USC-Information Sciences Institute, January 2006.

[CM07] E. Cumberbatch, and H. Morris, The gate to base capacitance of a MOSFET by asymptotic analysis. Discrete and Continuous Dynamical Systems - Series B, vol. 7, no. 3, May (2007).

[CUA07] E. Cumberbatch, S. Uno, and H. Abebe, Nano-scale MOSFET device modelling with quantum mechanical effects. Euro Jnl of Applied Mathematics(2007), vol. 17, p1-25.

[CWK96] K. Chen, H. Wann, and P. Ko, The Impace of Device Scaling and Power Supply Change on CMOS Gate Performance. IEEE, vol. 17, no. 5, p202-204, (1996).

[DPS03] K. Dragosits, V. Palankovski, and S. Selberherr, Mobility Modeling in Presence of Quantum Effects. IEEE, vol. 17, no. 5, p271-274, (2003).

[KC96] J. Kevorkian and J. D. Cole, Multiple scale and singular perturbation methods. Applied Mathematical Sciences vol. 114, Springer-Verlag, May (1996).

[MCPH00] H. C. Morris, E. Cumberbatch, T. Phillips, and B. Hinderberger, Analytical results for the current-voltage characteristics of an SOI-MOSFET. Proceedings, Third International Conference on Modeling and Simulation of Microsystems, San Diego, CA, March (2000).

[MA04] H. C. Morris and H. Abebe, MOSFET analytical substrate current model for circuit simulation. Proceedings (2004) International Conference on Computing, Communications and Control Technologies: CCCT'04,Vol. 1, pp. 162-165, Austin, Texas, USA.

[N02] A. Nadim, E. Cumberbatch, A. Attiyah, V. Dang, C. Mutlugun, C. Sabol and C. Wong, Gate capacitance modeling. Claremont Graduate University and USC/ISI Mathematics Clinic report, (2002).

[RAHKFG07] R. Rios, N. Arora, C. Huang, N. Khalil, J. Farcicelli and L. Gruber, A Physical Compact MOSFET Model, Including Quantm Mechanical Effects, for Statistical Circuit Design Applications. Digital Equipment Corporation, IEEE, April (2007).

[VWW94] M. Van Dort, P. Woerlee and A. Walker, A Simple Model for Quantization Effects in Heavily-Doped Silicon MOSFETs at Inversion Conditions. Solid-State electr., vol. 37, pp411-414, March (1994).

[WOC90] M. J. Ward, F. M. Odeh and D. S. Cohen, Asymptotic methods for metal oxide semiconductor field effect transistor modeling. SIAM J Appl. Math, vol. 50, No. 4, pp. 1099-1125, Aug (1990).

[W92] M. J. Ward, Singular perturbations and a free boundary problem in the modeling of field- effect transistors. SIAM J. Appl. Math. 52, pp. 112-139,(1992).